EVALUATION AND PERFORMANCE OF RAMMED AGGREGATE PIERS AND STONE COLUMNS IN SOFT CLAYEY SOILS

Jorge Badillo[1], Álvaro Pazmiño[1], Xavier Vera-Grunauer[2], Fausto Molina-Gómez[3], Kyle Rollins[4]

[1]ESPOL-FICT, Guayaquil, Ecuador

[2]Geoestudios S.A., Guayaquil, Ecuador

[3]CONSTRUCT-GEO, Universidade do Porto (FEUP), Porto, Portugal

[4]Brigham Young University

ABSTRACT:

Rammed Aggregate Piers® (RAP) and Stone Columns by vibro replacement (SC) are among the methods used for the construction of vertical gravel elements, increasingly employed as ground soil improvement techniques. This study describes and analyzes the performance of 41 RAP elements and 12 SC elements (53 in total) installed in two wastewater treatment plants (WWTP), located in the north and south of the city of Guayaquil (Ecuador), specifically along the banks of the Daule and Guayas rivers, respectively. The analysis includes geotechnical characterization generated through the interpretation of in-situ and laboratory tests, along with load tests and settlement plates, to provide design recommendations for ground improvement of alluvial and deltaic estuarine deposits, consisting of high plasticity, diatomaceous, naturally cemented clays with alternating seams of fine sands and silty sands stratum. The results revealed that the installation technique of vertical gravel elements and the soil matrix affect the ultimate bearing capacity, deformation modulus, and stiffness of the vertical elements, as well as the geotechnical properties of the soil matrix.

KEY WORDS:

Ground improvement, Rammed Aggregate Pier, Stone columns, Load test.

INTRODUCTION

Gravel columns were first utilized in France in 1830 to improve a soft soil site (Hughes & Withers, 1974). This technique gained widespread adoption in Europe from the 1950s following the development of the vibroflotation construction method in Germany. However, it wasn't until the 1970s that this practice was introduced in the United States (Barksdale & Bachus, 1983; Mitchell, 1981). Rammed Aggregate Piers were introduced to the market in the early 1990s. The soil improvement with vertical gravel elements is employed to increase bearing capacity (Han, 2015), increase slope stability (Parra et al., 2007; Wissmann et al., 2002), reduce and accelerate settlements due to consolidation in saturated fine-grained soils (Mohamedzein & Al-Shibani, 2011; Thompson et al., 2009), furthermore, these elements allow reducing the potential for liquefaction and its effects on saturated coarse-grained soils. (Adalier & Elgamal, 2004; Tiznado et al., 2021; Girsang et al., 2004; Rayamajhi, Ashford, et al., 2016; Rayamajhi, Boulanger, et al., 2016; Thum et al., 2021; Vera-Grunauer et al., 2019; Zalachoris et al., 2023).

Studlein & Holtz (2013) indicate that although there is a wide range of available installation techniques for vertical gravel elements, the performance of these techniques is indifferent to the construction method. Furthermore, these authors mention that despite advances in vertical column construction, certainty in predicting bearing capacity has not been satisfactorily established.

In Ecuador, the soil improvement technique with vertical gravel elements is an uncommon construction method, while the method of Rammed Aggregate Piers was introduced in the country in the last 10 years (Vera-Grunauer et al., 2017, 2019). Additionally, no studies have been conducted to verify the efficiency or performance of vertical gravel elements using different construction methods in soft clayey deposits in alluvial and deltaic estuarine environments. In Guayaquil, the presence of compressible soft soils, potentially liquefiable sands strata, shallow water levels, and high seismic hazard, necessitate understanding and comprehending the performance of vertical gravel element construction systems as soil improvement techniques.

Ng & Tan (2015) affirm that the drainage capacity of vertical columns could degrade due to the installation of the elements, causing soil disturbance around them, referred to as the "*smear zone*". The effect of reduced permeability around the vertical columns in the smear zone is an important factor for evaluating settlements when using vertical drains (Bergado et al., 1991). Indraratna et al. (2013), Pal & Deb (2019) y Tai & Zhou (2019) demonstrated that the obstruction effect around the vertical columns significantly reduces the drainage capacity of the elements, leading to a slower consolidation rate. Han & Ye (2002) proposed a simplified theoretical model to consider the effect of the smear zone on the radial coefficient of consolidation around granular columns, similar results were found in this study, for the alluvial and deltaic estuarine clays with sensitivities ranging from 2 to 20, where soil remolding effect develops around the perimeter of the RAP, significantly reduced the settlement rate.

Stuedlein & Holtz (2012) have conducted field studies to evaluate the individual performance of rigid vertical columns considering different construction processes, concluding that the performance of such techniques is indifferent to the construction method. However, Kwong et al. (2002) indicate that the effectiveness of the RAP system is attributed to the increase in lateral stress in the soil matrix during installation. Nevertheless, Handy & White (2006) suggest that transient liquefaction of saturated soil near the pile could occur if the lateral stresses exerted by ramming exceed the soil's compression strength based on K_0 measurements near RAP. Additionally, Halabian & Shamsabadi (2015) indicate that the construction process of rammed aggregate piers has a significant effect on the column behavior after conducting hybrid numerical analyses where they manage to capture the effect of the construction process in the model, showing the development of a radial expansion in the soil-column, altering the horizontal stress path, and resulting in an increase in horizontal stress reaching the passive limit state.

Zalachoris et al. (2023) conducted dynamic field tests in New Zealand and numerically modeled the experiments to assess the effect of RAPs on the performance of liquefiable silty sands or sandy silts. These authors demonstrated that soil densification around RAP elements and the increase in lateral earth pressure within the densified soils were the main soil improvement mechanisms contributing to the reduction of cyclic shear deformations and the generation of excess pore pressure during seismic loading. They also identified that the permeability and shear stiffness of the installed RAP did not have a significant influence on the response of pore pressure and shear deformations developed across the improved area. Although these studies were conducted in sandy silts and silty sands, with fines content ranging from 3 to 74%, the soil matrix improvement mechanism with diatomaceous clayey soils and intercalations of sands could be similar, where its efficiency depends on the hydraulic conductivity of the soil matrix. One way to estimate this effect is through the execution of pore pressure dissipation tests from cone penetration test device (CPTu), which allow obtaining the horizontal consolidation coefficient directly in the field. Finally, the findings by Zalachoris et al. (2023) confirm what Handy (2001) presented, mentioning that the construction process of RAP increases the horizontal soil pressure.

The objective of this work is to evaluate the performance of the vertical gravel elements installed using the RAP and SC methodology in the northern and southern WWTPs (Guayaquil, Ecuador), through the analysis of geotechnical exploration results, in-situ tests, and load tests to provide design recommendations for the improvement of soft clayey soils with deposition environments like this study. Additionally, this work presents the results of 53 load tests in soft soils. Finally, empirical equations are developed to estimate parameters for practical application in the calculation of load capacity in RAP and SC elements, where they are related to CPTu tests, which are widely accepted in the characterization of soft soils. The equations obtained represent the contribution of this research to the state of the art and practice in soil improvement, as there are no studies that relate load capacities in RAP and SC with parameters from the CPTu test. Additionally, the performance of two different construction methodologies for the installation of vertical columns as soil improvement (Stuedlein & Holtz, 2012) is evaluated at the same site, clearly observing different performances. Finally, the effect of improving the load capacity and stiffness of RAP with the replacement of existing soil through imported material with compacted gravel and clayey sands at 95% of the modified Proctor, at a depth of 3D from the surface is demonstrated, this improvement effect has not been documented in the technical literature through field tests.

MATERIALS AND METHODS

Description of experimental sites

Northern and Southern WWTPs

The city of Guayaquil is located on the banks of the Daule River and the Guayas estuary (Ecuador, South America). This city was urbanistically developed in flood-prone areas of alluvial plains in the north and estuarine delta plains in the central and southern regions due to tidal changes. The northern

WWTP is located north of Guayaquil next to the Daule River and will serve more than 1.5 million inhabitants. This represents the construction of the largest Rammed Aggregate Pier (RAP) in the country with 37,168 vertical elements and approximately 0.56 million meters of RAP. On the other hand, the southern WWTP is located south of Guayaquil, 200 meters from the Guayas estuary, and serves more than 1 million inhabitants. The construction included over 15,000 stone columns (SC) installed using the vibro replacement methodology. **Figure 1** shows the spatial location of the two study sites on the geotechnical zoning map of the city of Guayaquil, modified from Vera-Grunauer (2014).

In the northern WWTP, soil improvement consisted of installing Rammed Aggregate Piers with a length of 15 meters, a design diameter of 55 cm, triangular distribution, and spacing between axes ranging from 1.2 to 3.0 meters. The area above these elements would be filled with imported granular material up to the project level. Meanwhile, in the southern WWTP, soil improvement involved the installation of stone columns using vibro replacement with a length of 15 meters, a design diameter of 61 cm, triangular distribution, and spacing of 2.0 meters between axes. Similar to the northern WWTP, imported granular material would be filled over these elements. Since the vertical elements are long, it is expected that these elements will fail by bulging, a mechanism that occurs at depths of between 2 to 3 times the diameter. (Barksdale & Bachus, 1983); therefore, in the northern WWTP, a compacted granular improvement layer of 1.5 meters thick was placed from the head level in areas where soft clays were detected during the exploration stage, to provide greater lateral stiffness to the RAP. In areas where sandy clays or highly overconsolidated clays due to desiccation were detected, these were not replaced.

The northern WWTP is in geotechnical zone D4B, which corresponds to deposits of the alluvial plain of the Daule and Babahoyo rivers, see **Figure 1**. The southern WWTP is situated near zone D1, which corresponds to the deltaic estuarine deposits in the southeastern area of Guayaquil. The proportion of pyrite cementation present in the microstructure of the greenish-gray clays of the estuarine deltaic complex is the main difference from the alluvial clays found north of the city. However, diatoms were detected in the microstructure of the clays in both areas (GEOESTUDIOS S.A., 2015; Paredes, 2020; Vera-Grunauer, 2014). In zone D4B, the weathered sedimentary rock of the Cayo formation is found at shallower depths compared to the estuarine deltaic zone (D4B with soil thickness of 10-20 meters).

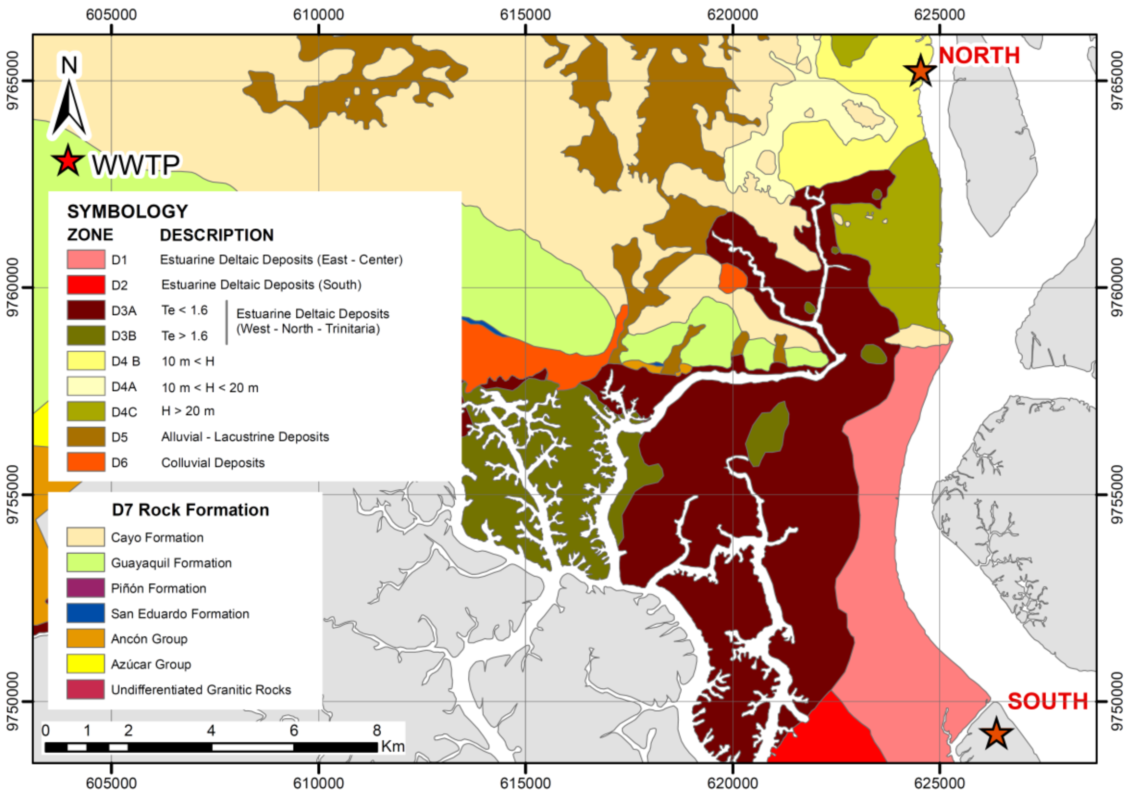

Figure 1. Northern and Southern WWTPs on the geotechnical zoning map of the city of Guayaquil, modified from Vera-Grunauer (2014).

Geotechnical Characterization

Geotechnical exploration includes, in the northern WWTP, 22 SPT tests conducted by Geoestudios, 61 SPT tests by Construladesa, and 16 CPTu tests with 20 pore pressure dissipation tests from CPTu, along with 3 estimations of shear wave velocities using MASW and 4 downhole tests from SCPTu test that measures shear wave velocities profiles. In the southern WWTP, 8 SPT tests were conducted by Geoestudios, 23 CPTu tests by Subterra, and 9 CPTu tests by Geoestudios. Supplementary materials show the implementation of geotechnical exploration at the 2 treatment plants. Additionally, 3 test sites with RAP elements were constructed in the northern WWTP, conducting SPT and SCPTu tests both within and outside of the improvement area. Through the measurement of normalized pore pressure (B_q), an estimation tendency to increases over time in OCR and K_0 were estimated in the clayey strata.

In **Figure 2 (a)** depicts the estimated subsurface stratigraphic profile of the northern WWTP, with horizontal axis showing distances every 20 meters and vertical axis indicating elevations in meters.

Section A-A' is oriented (W-E) towards the Daule River. Greenish clays (CH and CL) and clayey silts (MH and ML) were identified predominantly up to an elevation between -11 to -13 meters, followed by gray silty and clayey sands (SM, SC, and SP-SM) with lenses of fine-grained soils. The clayey and silty deposit exhibit rhythmic interbedding of sand layers. The median value of the first 15 meters of depth estimated from CPTu testing presents an undrained shear strength, S_u, ranging from 22 to 52 kPa and an overconsolidation ratio, OCR, from 1.1 to 2.0. Laboratory tests on clay samples estimated values at the 15-meter depth [median, maximum, minimum, coefficient of variation], sensitivity (St) of [4, 20, 2, 0.60] via the fall cone test, liquidity index (*LI*) of [1.60, 4, -1.2, 0.80], the ratio between water content and liquid limit (w_n/LL) of [1.3, 2.9, 0.1, 0.60], plasticity index (PI) of [45%, 58%, 20%, 0.20] and fine-grained content (FC) of [84%, 100%, 52%, 0.50]. Additionally, **Figure 2 (b)** presents the stratigraphic profile of the southern WWTP. Section B-B' is oriented (SW-NE) towards the Guayas estuary. A thick layer of soft clays (CH and CL) with sand's intercalations (SM and SC) was identified. The median value of the first 15 meters of depth estimated from CPTu testing presents a S_u ranging from 26 to 50 kPa and an OCR from 1.4 to 1.7. For the soft clay layer, laboratory tests were conducted, and values were found in the first 15m of depth [median, maximum, minimum, coefficient of variation], of LI of [0.70, 1.4, -0.1, 0.60], w_n/LL of [0.9, 1.2, 0.3, 0.50], PI of [40%, 60%, 20%, 0.25] and FC of [85%, 100%, 55%, 0.50]. As observed, both sites have similar median ranges of shear strength and OCR; however, the clays at the Northern WWTP site are more sensitive than the Southern WWTP site.

Robertson (2009, 2012) used critical state soil mechanics theory to define normalized undrained shear strength for the yield stress or preconsolidation stress ($S = S_u/\sigma'_y$). Equations 1 and 2 consider the mode of failure as undrained simple shear (DSS), $S = 0.5 \sin \phi'$, and the relationship under the concept of SHANSEP (Ladd & Foott, 1974), $S_u/\sigma'_{vo} = S*OCR^m$. The following equations have been considered for estimating S_u, OCR, and M from CPTu tests, according to Robertson (2009, 2012):

$$S_u=(q_t-\sigma_{vo}) / N_{kt};\ N_{kt}=10.50 + 7 \log (F_r);\ q_t = q_c + (1-a_{net}) * u_2;\ F_r (\%) = (100 f_s)/(q_t-\sigma_{vo}) \quad (1)$$

$$OCR=k_{OCR}*Q_{tn};\ k_{OCR}= [Q_{tn}^{0.20} / (0.25*(10.50+7\log (F_r)))]^{1.25}; \quad (2)$$

$$Q_t = (q_t-\sigma_{vo})/\sigma'_{vo};\ Q_{tn}= Q_t*(\sigma_{atm}/\sigma'_{vo})^n \quad (3)$$

If $I_c > 2.2$, $M = \alpha_M (q_t - \sigma_v)$; $\alpha_M = 14$ for $Q_{tn} > 14$ & $\alpha_M = Q_{tn}$ for $Q_{tn} \leq 14$ (4)

If $I_c \leq 2.2$, $M = (q_t - \sigma_v) * 0.0188 * 10^{0.55 I_c + 1.68}$; $I_c = ((3.47 - \log Q_{tn})^2 + (\log F_r + 1.22)^2)^{0.5}$ (5)

Construction of Gravel Vertical Elements (RAP & SC)

The construction of vertical gravel elements may involve displacement or pre-excavation of the surrounding soil, as well as densification of the surrounding soil and improvement aggregate by vibration or ramming. For the installation of RAP elements, a displacement and ramming system patented by Geopier called "*Impact*" was adopted. The system uses an excavator incorporating a vibratory hammer along with a displacement mandrel and a high-frequency rammer. The mandrel is inserted into the soil with a static force of 200 to 300 kN, augmented by dynamic vertical impact energy. The system includes a device (steel chains) at the tip of the tube that prevents soil from entering it as it penetrates the ground. After inserting the tube to the design depth, the granular aggregate is placed, then the tube along with the rammer is lifted approximately 0.91 m (3 feet), and 0.60 m (2 feet) is rammed in to form a compacted layer 0.30 m thick, with a compaction pressure of 17 MPa. This process is repeated successively until reaching the design head elevation. The RAP elements were installed by 3 different work fronts throughout the construction process.

The stone columns (SC) were constructed using vibro replacement, which involved driving an APE 200-6 hammer with a force of up to 3020 kN into the ground through a steel casing with a diameter of 0.42 m, which is introduced by vibration with a frequency of up to 1650 rpm to the design depth. Subsequently, gravel is introduced into the empty casing using an excavator that fills a hopper with a capacity of 4.2 m^3, which is equipped with windows through which the gravel enters the injector. Then, the injector is extracted through the vibration process, allowing the gravel to occupy the empty space left by the casing. This process is carried out at intervals of approximately 0.40 m, generating a cyclic work of extraction and re-driving. Compaction is provided to the gravel at each re-driving of the casing, forming the columns. Water was necessary during the procedure to balance the hydrostatic pressures of the gravel and the soil.

In the Northern WWTP, the effective consumption and nominal diameter of 2808 reported RAP elements have been evaluated, with an average diameter of 58 cm and a coefficient of variation of 2.4%.

Load test and Geotechnical instrumentation

The load tests involve applying incremental compression loads using a hydraulic jack, with the reaction element being the pile driver or a loaded dump truck. The hydraulic jack was positioned on a concrete pad with a thickness ranging from 0.40 to 0.50 m cast on top of the element. Subsequently, deformation gauges were installed to record vertical deformation at each load increment. Loading and unloading were performed for each test, with the application time of each load increment varying from 24 to 36 minutes. At the Northern WWTP, the maximum load applied to the test elements was 309 kN, while at the Southern WWTP, it was 152 kN. **Figure 3 (b)** illustrates the setup of a load test conducted at the Northern WWTP, also showing in **Figure 3 (a)** the proximity of the study area to the Daule River.

In the Northern WWTP, 40 load tests on RAP elements with and without granular fill in the first 1.5 m of the column are presented. Meanwhile, in the Southern WWTP, 12 load tests on SC and 1 load test on RAP are presented. This demonstrates the application of two installation methods in the same construction project, highlighting the importance of this comparison in engineering practice and soft soil improvement.

Figure 4 presents the results of tests conducted on RAP elements with 1.5 m improvement from the head of the element at the Northern WWTP (RAP+FILL1.5 m, Northern WWTP), tests conducted on RAP elements with natural soil at the Northern WWTP (RAP+NAT.SOIL, Northern WWTP), tests conducted on SC elements at the Southern WWTP with natural soil (SC+NAT.SOIL, Southern WWTP), and tests conducted on RAP element at the Southern WWTP with natural soil (RAP+NAT.SOIL, Southern WWTP). In **Figure 4 (a)** and **(b)** the vertical deformations measured during the tests were normalized for the element diameter. By selecting the variables qg and kg for the same normalized deformation from **Figure 4 (a)** and **(b)**, respectively, **Figure 4 (c)**. is obtained. Evaluating the mean of all stiffness curves, kg, it is observed that by placing the granular fill at a depth of 3D from the head of the RAP, the stiffness of the RAP increases by 50% compared to RAP in natural soil, ($k_{gRAP+FILL}/k_{gRAP+NAT.SOIL}=1.5$), for small deformations $\delta/D \leq 0.01\%$, Additionally, it is observed that this effect decreases with increasing normalized deformation, reaching a stiffness ratio of ($k_{gRAP+FILL}/k_{gRAP+NAT.SOIL}$=1.2), for $\delta/D \leq 10\%$. Comparing the mean for the condition of RAP and SC in natural soil, a nearly constant ratio is observed for $0.01\% \leq \delta/D \leq 10\%$ of $k_{gRAP+N.SPOIL}/k_{gSC+NAT.SOIL}$=2, meaning a 100% increase of stiffness. This reaffirms that the construction system and the lateral stiffness condition, at least at 3D depth, greatly influence the stiffness of the vertical gravel element.

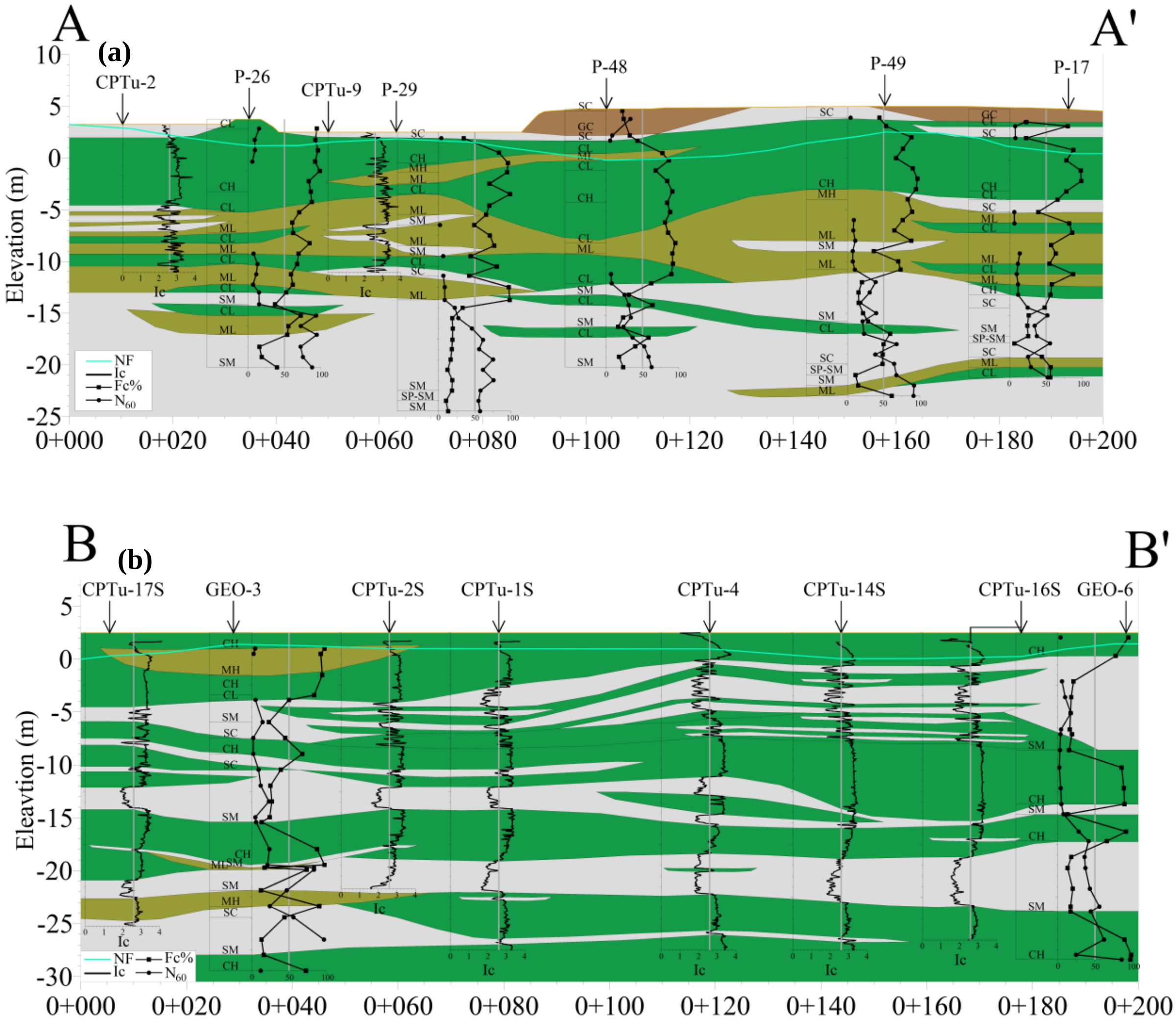

Figure 2. Estimation of subsurface stratigraphic profiles in the studied areas: (a) Northern WWTP; (b) Southern WWTP.

Figure 3. Configuration of a load test for the RAP during the study phase, Northern WWTP: (a) view of the Daule River and the equipment for installing the RAP, and (b) the test setup.

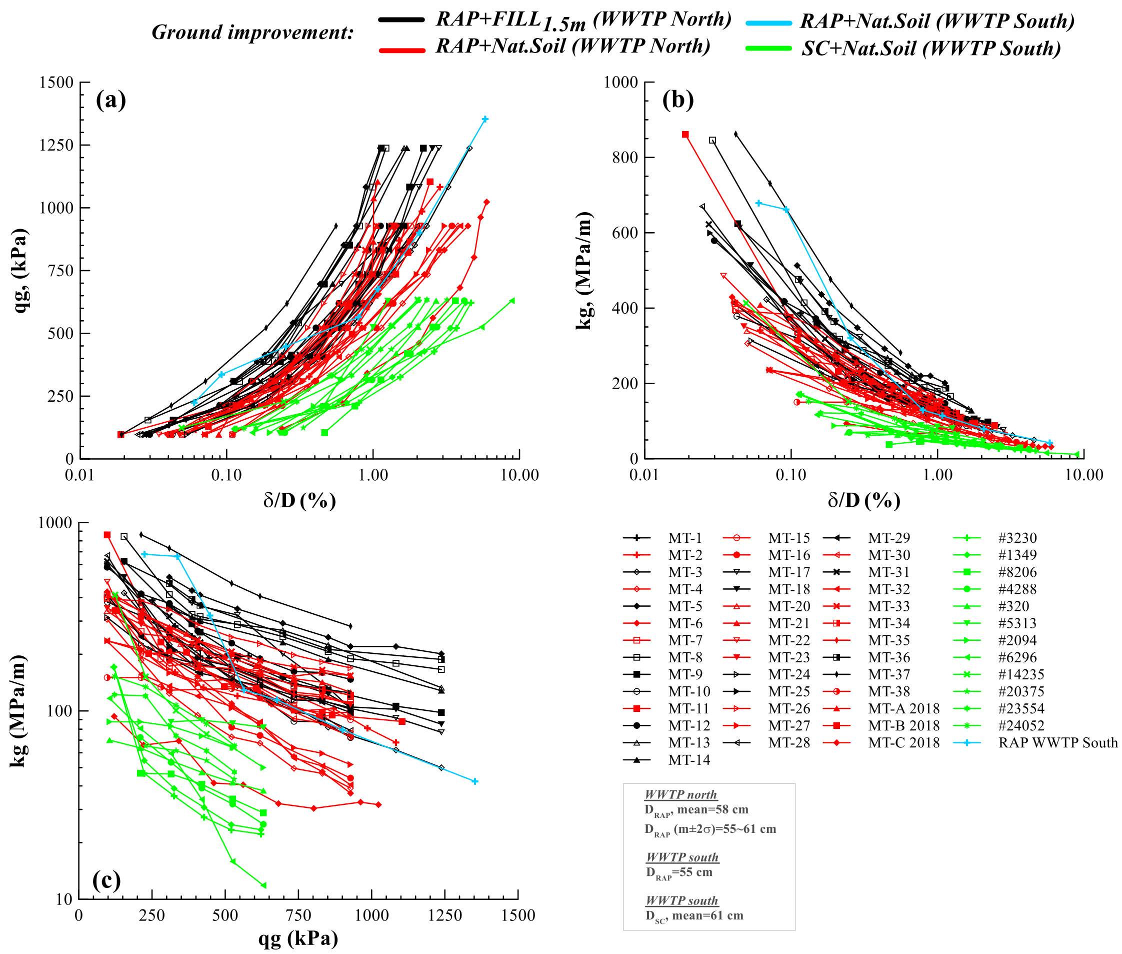

Figure 4. Results of the load test. (applied stress at the head (q_g) vs. normalized deformation (δ/D). (b) stiffness (k_g) vs. normalized deformation (δ/D). (c) stiffness (k_g) vs. applied stress at the head (q_g).

Load tests in Southern WWTP

Once the mean values of the trends from all the load tests conducted at the two study sites were evaluated, the performance of the vertically installed columns by ramming (RAP) and vibro replacement (SC) was assessed at the same site (Southern WWTP). In **Figure 5 (a)** applied stress at the head, q_g, is presented with normalized deformation, in **(b)** k_g is presented with normalized deformation, in **(c)** the relationship between k_g and q_g is presented, and in **(d)** the ratio between the k_g values obtained from RAP and SC construction methods is presented, for the mean stress at the head of the vertical element, q_g. In **Figure 5** the load test on the RAP element called RAP Southern WWTP and the load tests on the SC elements called #23554 and #24052 were considered. Additionally, load test data on a column installed using the Geopier methodology (non-impact), element (GP) with a diameter of 76 cm, and (SC) element with a diameter of 91 cm shown in White et al. (2002) are included.

In **Figure 5 (a)** it is observed that for the same stress, higher deformations were reported in the (SC) elements. In **Figure 5 (b)** it is observed that for the same normalized deformation, the stiffness is higher in the (RAP) element; this trend decreases with the increase of the normalized deformation. In **Figure 5 (c)** it is observed that the rate of increase in stiffness of the elements decreases with the stress demand at the head of the elements. Finally, in **Figure 5 (d)** the relationship between the stiffness of the RAP and SC elements is presented, with an estimated mean of 4.0 to 5.5, along with the data reported by White et al. (2002) of 7.8. It is important to recognize that subsurface geotechnical parameters have a significant influence on the performance of the elements; therefore, the geotechnical characteristics of the two sites where the load tests were conducted were evaluated, as shown in **Table 1.**

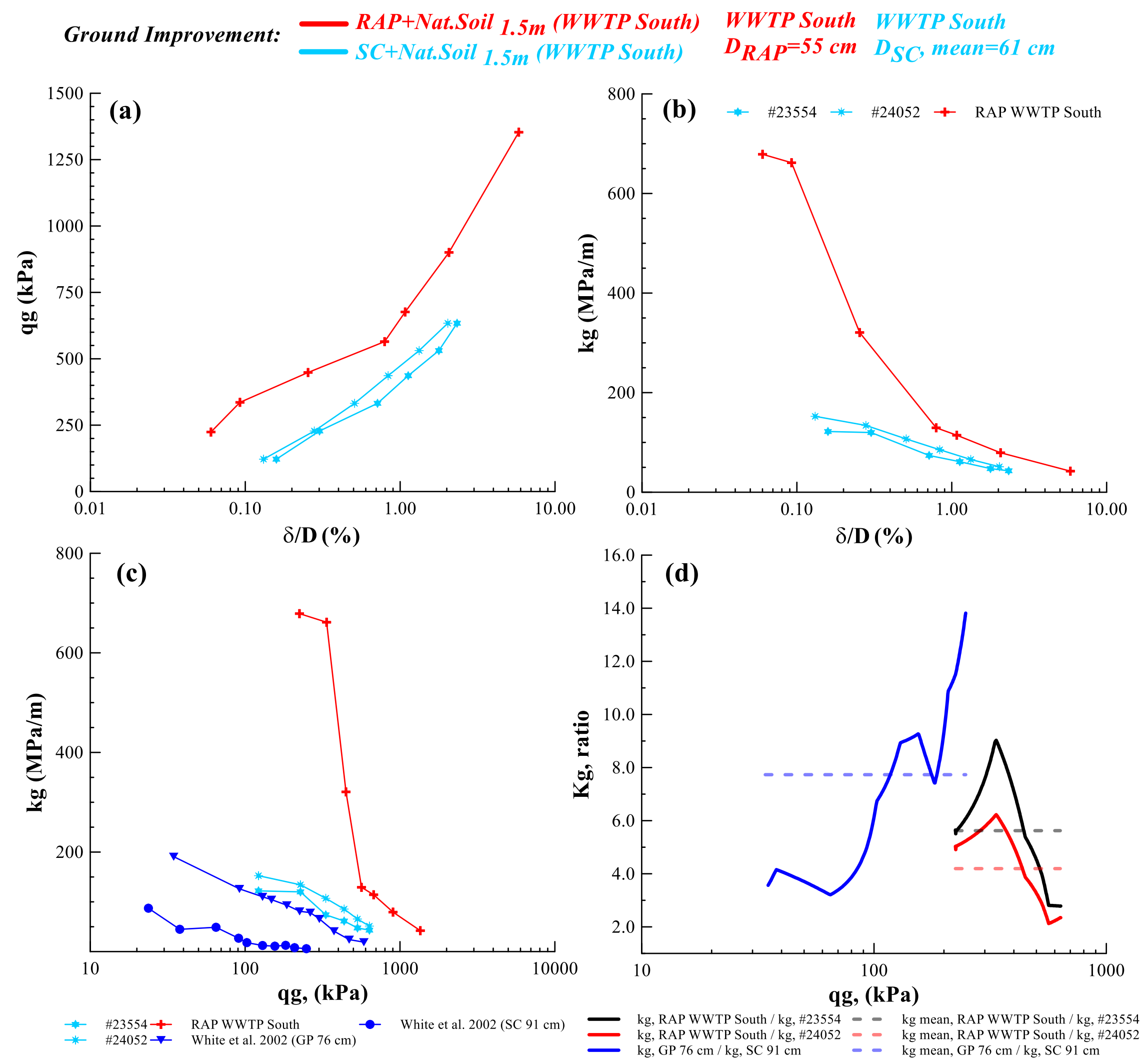

Figure 5. Load test results: RAP and SC (#23554, #24052) in Southern WWTP. (a) q_g vs. normalized deformation (b) k_g vs. normalized deformation. (c) k_g vs. q_g. (d) relationship between the stiffness of RAP and SC for various stress levels at the head q_g, as well as the results reported by White et al. (2002).

Table 1 presents a summary of the geotechnical parameters of the subsurface prior to the installation of the elements. The clay layer until 3m depth, around the RAP Southern WWTP load test, exhibits a geometric mean of S_u from 25 to 26 kPa, and OCR from 2.6 to 3.6, while the clay layer until 3m depth around tests #23554 and #24052 (SC), exhibits a geometric mean of S_u from 24 to 28 kPa, and OCR from 2.8 to 3.0. Overall, the two sites have the same geotechnical characteristics prior to the installation of the elements. As result, it could be considered that the increase in stiffness and load capacity of the rammed aggregate pier (RAP), compared to the one built by vibro replacement (SC) are due to the combined effect between the behavior of the element because radial expansion occurs during the construction of the RAP and the change or improvement of the geotechnical characteristics in the surrounding soil, where the effectiveness of the improvement depends on the overall hydraulic conductivity of the soil matrix. The results of the Southern WWTP and those reported by White et al. (2002), which correspond to load tests with two different construction methods in sites with the same geotechnical characteristics, contradict what was found by Stuedlein & Holtz (2012), where they indicate that the performances of the pressure-deformation relationship in shallow foundations with vertical gravel elements were insensitive to the method of construction, considering various aggregate gradations and compaction methods.

Table 1. Summary of geotechnical parameters of the subsurface at the Southern WWTP load test sites for RAP and SC elements.

WWTP:	**South**		**South**	
Vertical Elements:	**RAP**		**SC**	
ID:	RAP WWTP South		#23554	#24052
Date:	21/8/2015		26/4/2019	26/4/2019
S (m):	2.0		2.0	2.0
D (m):	0.55		0.63	0.61
L (m):	13.0		15.0	15.0
Borehole:	CPTu1 fuera	CPTu16 S	CPTu2 S	CPTu17 S
Ic (3m):	2.62	2.72	2.85	3.02
Ic (15m):	2.82	2.71	2.92	3.10
qt, MPa (3m):	0.63	0.57	0.57	0.47
qt, MPa (15m):	1.07	1.32	0.91	0.75
Fr, % (3m):	3.99	3.21	4.60	5.73
Fr, % (15m):	3.30	2.36	3.14	3.69
Su, kPa (3m):	26.22	25.52	28.02	23.93
Su, kPa (15m):	44.43	49.60	39.57	35.22
OCR (3m):	3.67	2.64	3.77	2.85
OCR (15m):	1.80	1.69	1.70	1.39

RESULTS ANALYSIS AND DISCUSSION

Performance of the vertical gravel elements

Ultimate load capacity

The load tests conducted on the vertical gravel elements aimed to determine the variation of stiffness for the stress at the head, and these did not reach the maximum load or failure of the elements. The test results were used to estimate the ultimate load capacity by extrapolating the calibrated trend of the stress-strain relationship using the hyperbolic method (Duncan & Chang, 1970; Kondner, 1963). Lutenegger & Adams (1998) evaluated various graphical methods to estimate ultimate load capacity in load tests, ultimately recommending the hyperbolic method (Cadden et al., 2004; Stuedlein & Holtz, 2013) . As such, the vertical deformation measured was normalized for the element diameter (δ/D), thus obtaining stress at the head curves, q_g, and normalized deformation, which allowed grouping the results for each group of vertical gravel elements. In equation (6), the variables *a* and *b* are shown, defined in **Figure 6**, where q_f represents the ultimate capacity, considering an R_f value of 0.98.

$$q_g = \frac{\left(\frac{\delta}{D}\right)}{a+b\left(\frac{\delta}{D}\right)} \tag{6}$$

In **Figure 6 (a)** the results of the MT-9 load test and the model calibration are shown, and in **Figure 6 (b)** the determination of variables *a* and *b* is depicted. This procedure was applied for each load test, from which the following were obtained: q_{ult}, E_{50}, k_g and (δ/D) at 50% of the ultimate load capacity, FS=2.

The secant modulus at 50% of q_{ult}, can be obtained as follows:

$E_{50\ [RAP/SC]}= k_{g,\ FS=2}*4D$, where D is the diameter of the element in (m), k_g in (MPa/m). (7)

$E_{50\ [RAP/SC]}= \frac{q_{ult}}{5\left(\frac{\delta}{D}\right)_{FS=2}}$, q_{ult} in (KPa), δ/D in (%), E_{50} in (MPa). (8)

The value of 4D represents the depth at which resistance mobilization and deformation occur due to the failure mechanism in long vertical elements, according to Datye (1982) , which is typically 3 to 4 times the diameter (D). In calibrated numerical models with load tests, values from 4.0 to 4.3D were obtained in this study. As the deformation E_{50} is related to the major principal or vertical stress, σ'_1 and M (E_{oed}, oedometric module) is related to the confining stress, σ'_3, the stress ratio is given by $\sigma^{ref}{}_{oed} = \sigma^{ref}/K_o{}^{NC}$, and the modulus ratio is $M^{ref}/E_{50}{}^{ref} = K_{o,NC.}$ From the results of the CPTu tests and the normalization of the resistance, an S = 0.20 was estimated, representing a ϕ'_{DSS}=22º or the DSS test estimated with CPTu.

Vera-Grunauer (2014) presented DSS test results in the gray-green clays of Guayaquil with ϕ'_{DSS} from 20° to 25°. Therefore, $E_{50ref} = M_{ref}/K_{o,NC}$, $E_{50ref} = 1.6 * M_{ref}$, ref= 100 kPa.

In the supplementary materials is presented the information and summary of results for the load tests. **Figure 7** graphically presents the summary of results for each construction methodology, observing the mean values and graphically in the rectangle, the values of the 25th and 75th percentiles, as well as the minimum and maximum thresholds of each variable.

Shields et al. (2004) presented the results of 19 load tests on RAP in loose to very dense sandy soils (SM/SC, SM, SP), where the mean stiffness modulus, k_g, was 184 MPa/m for stresses at the head of the elements (at the inflection point of the stress-strain curve), with minimum and maximum values from 60 to 417 MPa/m, respectively. Additionally, the mean secant modulus for the same stress at the head of the RAP was 533 MPa, with minimum and maximum values of 131 to 2087 MPa, respectively. For RAP+FILL, in **Figure 7 (b)** a value of 419 MPa is observed for the mean E_{50}, and in **Figure 7 (c)** a value of 180 kPa/m is observed for the mean $k_{g,FS=2}$ (stiffness modulus). From the observations, the mean, minimum, and maximum values of each parameter are similar to those reported by Shields et al. (2004) in granular soils, which are equivalent to RAP elements installed with granular improvement material at a depth of 3D. From the mean values of the parameters for each construction system, it is obtained that the ultimate load capacity ratio of RAP+FILL/RAP+NAT.SOIL is 1.12 and of RAP+NAT.SOIL/SC+NAT.SOIL is 1.44. For the E_{50} the ratio of RAP+FILL/RAP+NAT.SOIL is 1.50 and the ratio of RAP+NAT.SOIL/SC+NAT.SOIL is 2.14. For the $k_{g,FS=2}$ modulus, the ratio of RAP+FILL/RAP+NAT.SOIL is 1.48 and the ratio of RAP+NAT.SOIL/SC+NAT.SOIL is 2.27. Finally, an increase of 33% in the normalized deformation of RAP+NAT.SOIL with respect to RAP+FILL was identified, while an increase of 58% in the normalized deformation of SC+NAT.SOIL with respect to RAP+NAT.SOIL. From the presented results, a superior performance of RAP is observed when laterally confined, at least 3D in depth, with selected granular material fill (SM, SC, GC) compacted to 95% of modified Proctor.

For the vertical gravel elements constructed with RAP, a ratio of $E_{50} \approx 2.3\ k_{g,FS=2}$ was determined, and for the SC elements, a ratio of $E_{50} \approx 2.45\ k_{g,FS=2}$.

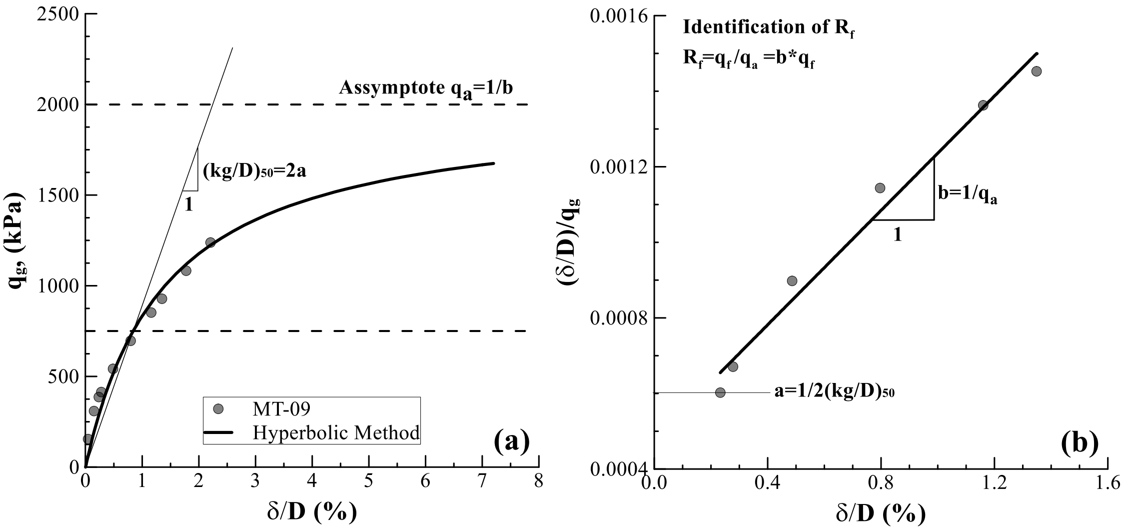

Figure 6. Determination of q_{ult} using the hyperbolic method for test MT-9.

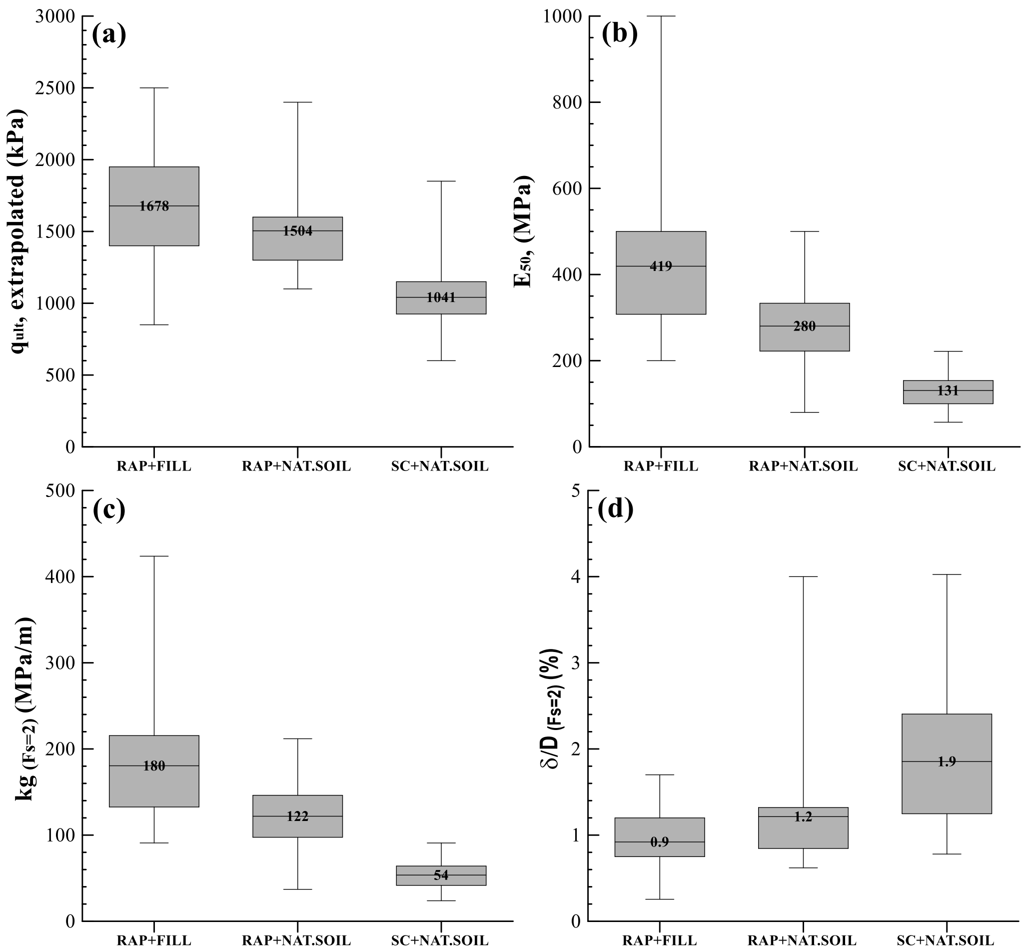

Figure 7. Summary of parameter results by construction methodology. (a) Extrapolated q_{ult}, (b) E_{50} of the vertical gravel element, (c) k_g at 50% d of ultimate capacity, and (d) normalized deformation at 50% of ultimate capacity.

Stiffness and deformations of individual gravel columns

From the processed information of 53 load tests, a statistical analysis was conducted for each type of tested vertical gravel element to estimate the mean variation of the element stiffness (k_g) with normalized deformation (δ/Diameter of the element), as shown in **Figure 8 (a)**. Additionally, a bi-normalized curve is presented in **Figure 8 (b)** where the stress at the head of the element is normalized to the extrapolated ultimate load capacity and the vertical deformation with the diameter of the element, obtaining equations of mean trends and the variation of COV (standard deviation/mean). With the mean of the bi-normalized curves, the following expressions were obtained:

For RAP+ FILL, RAP with lateral granular fill, the mean relation of

$$q_g/q_{ult} = 0.457(\delta/D)^{0.45}, \text{ with } COV_{mean} = 0.17 \quad (9)$$

For RAP+ NAT.SOIL, RAP with natural soil, the mean relation of

$$q_g/q_{ult} = 0.397(\delta/D)^{0.43}, \text{ with } COV_{mean} = 0.23 \quad (10)$$

For SC + NAT. SOIL, SC with natural soil, the mean relation of

$$q_g/q_{ult} = 0.362(\delta/D)^{0.43}, \text{ with } COV_{mean} = 0.25 \quad (11)$$

Estimating q_{ult} with the equations presented in the following section and considering the variability of the estimation [m*(1±COV)], stiffness curve could be determined varying with the vertical deformation of the element. If the relationship between the mean trends obtained is evaluated, it is shown that the stiffness of the elements (RAP+FILL) is greater compared to the elements (RAP+Nat.Soil) and (SC+Nat.Soil). It can be perceived that for the same construction method (RAP+FILL) vs (RAP+Nat.Soil), the increase in element stiffness varies from 1.2 to 1.5, the former at large deformations and the latter at small deformations, this is because, at a depth of 3 times the diameter of the element, bulging failure predominates. Additionally, comparing the stiffness between the two construction methods without fill, (RAP+Nat.Soil) and (SC+Nat.Soil), the stiffness increase is 1.9 to 2.0 times.

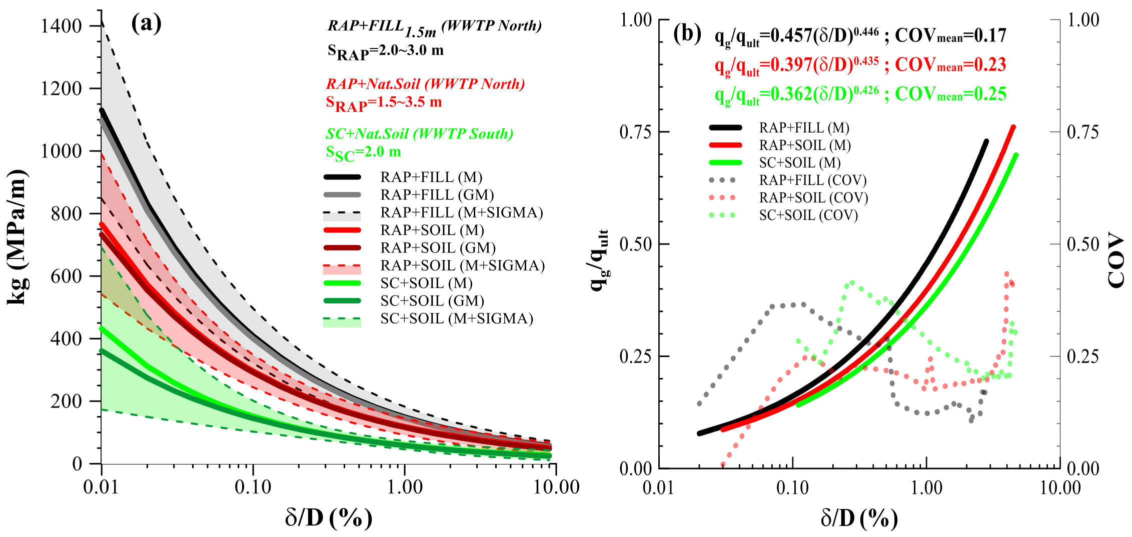

Figure 8. Variation of element stiffness with normalized vertical deformation (a) and the bi-normalized curve of head stress and deformation (b) for RAP and SC.

Estimation of ultimate load capacity

As mentioned earlier, the failure mode of a long vertical gravel element, with sufficient strength in the shaft and tip to prevent settlement, is called bulging, and it is governed by the ultimate radial confinement pressures or stresses and the shear strength of the surrounding soil matrix. In this work, the RAP and SC elements are long (L/D>20) which indicates that the failure mechanism is bulging. For the two construction systems of vertical gravel elements, an internal friction angle, ϕ'_p, de 45º has been considered, like Stuedlein & Holtz (2013). As recommended by Barksdale & Bachus (1983) for theoretical analyses between 38º to 45º.

Procedure 1 will be referred to as the empirical method proposed by Mitchell (1981), as shown in equation (12), where the ultimate load capacity of a unit element is proposed based on the theory of cylindrical cavity expansion by Vesić (1972),

$$q_{ult}= S_u*N_p \tag{12}$$

where N_p = load capacity factor. Mitchell (1981) recommends a value of 25. Barksdale & Bachus (1983) recommend N_p values between 18 to 22 for soils with low to high stiffness, respectively. Datye (1982) proposes for gravel columns constructed by vibro-replacement a range of 25 to 30, and for stone columns with vibro-displacement a range of N_p=40. Stuedlein & Holtz (2013) proposed an exponential equation based on undrained shear strength, shown with a blue line in **Figure 9**, and with a dashed line the logarithmic equation obtained in this study. Based on the results presented in supplementary materials, the relationship between N_p with S_u obtained from CPTu tests in the first 3D depth and the values reported by Stuedlein & Holtz (2013) are shown in **Figure 9**.

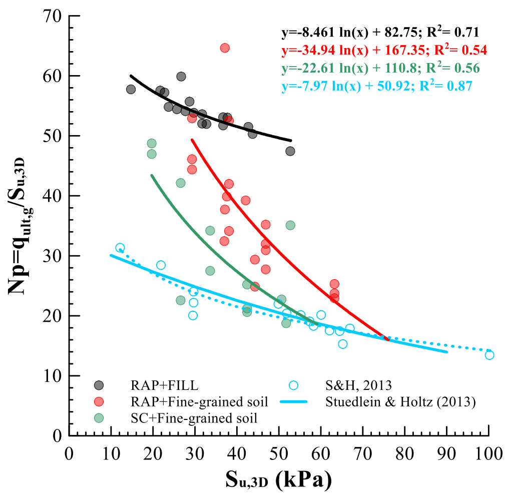

Figure 9. Relationship between N_p and undrained shear strength for the depth of 3D for the tested vertical gravel elements.

From the conducted statistical analysis, a relationship between N_p and $S_{u,3D}$ (kPa) is observed as follows:

$$N_p = \alpha - \beta \ln(S_{u,3D}) \tag{13}$$

The N_p values for laterally confined RAP with granular fill have a higher value compared to all other construction systems, demonstrating the good performance and efficiency of confining RAP in 3D to 4D with granular material. The trends of RAP+NAT.SOIL elements intersect with the trend of Stuedlein & Holtz (2013) at 75kPa and for SC+ NAT.SOIL at 55 kPa. For the same value of S_u the N_p value of RAP is always higher than that of SC. **Table 2** shows the constants of equation (13) for each vertical gravel element.

Table 2. Values of the constants of the logarithmic regression for the vertical gravel elements.

	α	β	R^2
RAP+FILL	82.75	8.461	0.71
RAP+NAT.SOIL	167.35	34.94	0.54
SC+NAT.SOIL	110.80	22.61	0.56
Stuedlein & Holtz (2023)	50.92	7.97	0.87

Procedure 2 is based on a multiple-variable linear regression analysis where the ultimate bearing capacity is normalized with the cone tip resistance q_t, meaning the relationship q_{ult}/q_t is estimated. For the case of RAP+FILL confined with granular fill, a fill angle ϕ of 38º is considered, typical for compacted clayey gravel or clayey sand fills. All geotechnical parameters (M in MPa, OCR, q_t in MPa) are estimated using the CPTu test and the previously described expressions, using the geometric mean at a depth of 3D, measured from the top of the element. The value of I_{r50} is estimated using the equation (20).

For RAP+FILL elements, the relationship of q_{ult}/q_t has an $R^2 = 0.985$ and a standard error of SE=0.029, where the expression ($4x10^6*I_{r50}^{-1.828}$) represents effective cohesion (in kPa) and the effective vertical stress at half the thickness of 3D, σ'v in kPa.

$$q_{ult\,(\mathrm{RAP+FILL})}/q_t = 0.764 - 0.000268*I_{r50} + 0.0193*[4x10^6*I_{r50}^{-1.828} + \sigma'v_{\,z=1.5D} \tan(38°)] \quad (14)$$

For RAP+NAT.SOIL elements, the relationship of q_{ult}/q_t has an $R^2 = 0.74$ and a standard error of SE=0.3.

$$q_{ult\,(\mathrm{RAP+SOIL})}/q_t = 2.682 - 0.155*M - 0.102*OCR + 0.0076*I_{r50} \quad (15)$$

For SC+NAT.SOIL elements, the relationship of q_{ult}/q_t has an $R^2 = 0.77$ and a standard error of SE=0.2.

$$q_{ult\,(\mathrm{SC+SOIL})}/q_t = 5.312 - 0.1694*M - 0.029*OCR - 0.0057*I_{r50} \quad (16)$$

To compare the results obtained from the load tests in this study, the equation proposed by Stuedlein & Holtz (2013) was considered. This equation is based on a modification of the ultimate bearing capacity (in kPa) of a gravel aggregate pile proposed by Hughes et al. (1975). The proposed equation is:

$$qult = [\sigma ro + [-1.45.\ln(S_u) + 8.52].S_u.\frac{1+sin\phi_p}{1-sin\phi_p}, \quad (17)$$

$$\sigma ro = \left(q + \frac{2S_u}{sin2\delta}\right)\left(1 + \frac{tan\delta_p}{tan\delta}\right) \quad (18)$$

Where σ_{ro} is the total radial in-situ stress, S_u is the undrained shear strength for the depth of 3D, ϕ_p es de 45º, q is the imposed load, in this case, it is zero, and $\delta_p = 45º + \phi_p/2$. For all types of vertical gravel elements, a δ of between 59 to 60° was obtained (COV= 0.02). For some years now, in projects with

RAP, the equation proposed by Wissmann (1999) has been recommended for estimating the ultimate bearing capacity per unit of RAP by bulging, equation (19). The effective vertical stress is considered at half the thickness of 3D, and the geometric mean of S_u in 3D, as shown in supplementary materials.

$$q_{ult}= 15.1\ \sigma'_v + 39.3 S_u, \qquad (19)$$

In **Figure 10 (a)** the estimation of the ultimate bearing capacity with the four procedures are shown for all construction systems of vertical gravel elements and the extrapolated value with the hyperbolic method for the load tests. In **Figure 10 (b)** the residual represented by the difference between the natural logarithm of the extrapolated value and the estimated value is shown. Additionally, in **Figure 10 (b)** the median residual for each vertical gravel element system has been calculated. It can be observed that the q_{ult}/q_t relationship obtained in this study (procedure 2) has the lowest median residual (-0.01, 0.04, -0.06). The equation proposed by Stuedlein & Holtz (2013) underestimates the ultimate capacity for RAP+FILL systems, i.e., it fails to capture the effect of the stiffness of the compacted granular material, represented by I_{r50} in equation (14), and overestimates the ultimate capacity for RAP and SC systems with NAT.SOIL (natural soil). The equation by Wissmann (1999) underestimates the ultimate bearing capacity in RAR+FILL systems, with lateral confinement of granular fill, and overestimates the capacity in RAP+NAT.SOIL systems when in natural soil. Caution should be exercised when using equation (19) when dealing with clayey soils at a depth of 3 to 4D.

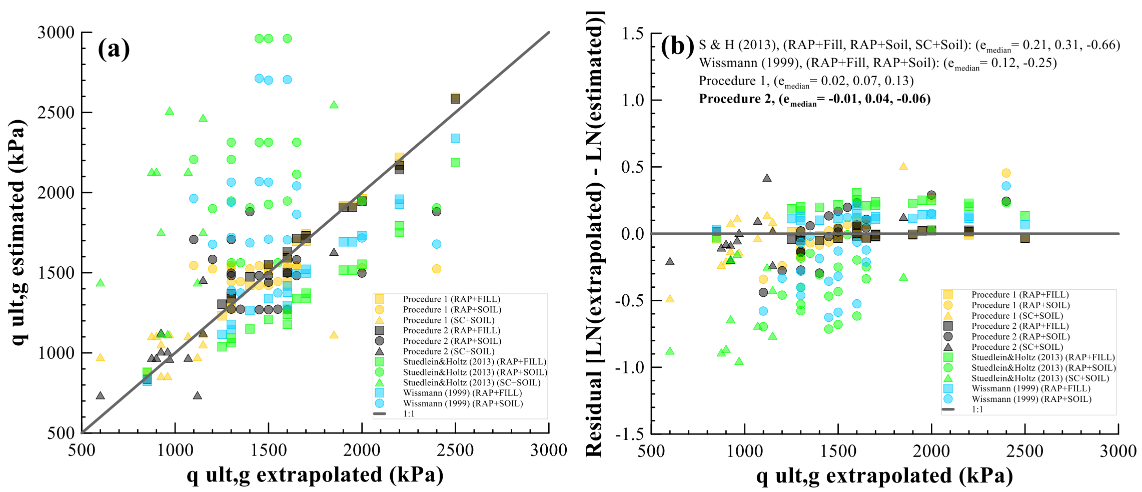

Figure 10. Comparison of the estimated and extrapolated ultimate bearing capacity values (a) in (kPa); (b) residual values in each procedure used in the estimation of the ultimate capacity.

In Equation (20), a linear regression model is presented for the clayey deposits from City Guayaquil for the estimation of the stiffness index, I_r, considering the values of the geometric mean within the thickness of the clayey layer. G_{max} was obtained from downhole tests from SCPTu (seismic cone penetration test) and G_{50} based on direct simple shear test results (Vera-Grunauer, 2014) where $G_{50}/G_{max} = 0.22$. **Figure 11** shows the comparison between the linear regression model and database from shear wave velocity measurements and CPTu tests for stiffness index estimations

$$\mathbf{I_{r,\,GM} = G_{50} / S_u} = 82.57 - 2.182 * S_u(kPa) + 17.85 * M(MPa) + 16.85 * OCR \tag{20}$$

$R^2 = 0.90$, SE=9.48; GM values @H_{soil}: [S_u, OCR, M] f(CPT), $15 \leq PI_{GM} \leq 41$, $S_{u,\,GM} \leq 60$kPa, $OCR_{GM} < 3$; n =53

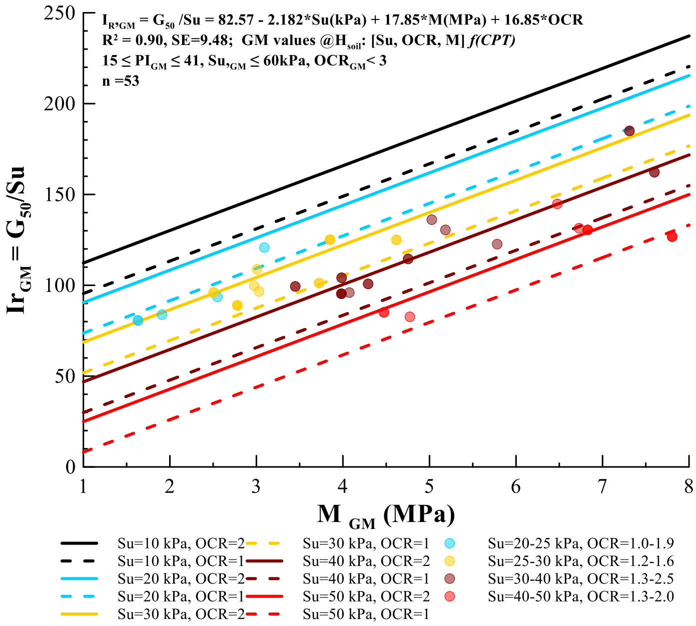

Figure 11. Comparison between the linear regression model and database from shear wave velocity measurements and CPTu tests for stiffness index estimations.

CONCLUSIONS

In very few soil improvement construction projects, two or more types of construction methodologies are tested, as in the case of the Southern WWTP site. In the case of the Northern WWTP site, 41 load tests were analyzed for RAP elements, and 12 load tests for SC elements at the Southern WWTP site. With the information analyzed and interpreted, several findings and practical recommendations in the design of vertical gravel elements in soft clayey deposits in alluvial and deltaic estuarine environments near riverbanks can be mentioned:

- The results shown in the Southern WWTP, where load tests were conducted using two different construction methods, RAP and SC by vibro replacement, at sites with the same geotechnical characteristics, demonstrate that the construction process does indeed influence the performance of vertical gravel elements, clearly contradicting what was stated by Stuedlein & Holtz (2013). The ratio between RAP and SC is, $q_{ult,\ \mathrm{RAP}}/q_{ult,\ \mathrm{SC}} = 1.7$, $E_{50,\ \mathrm{RAP}}/E_{50,\ \mathrm{SC}} = 1.4$ for $R_{s,3D}$ from 11 to 13, S/D =3.
- Considering that the CPTu test is commonly used in the practice of soft soil characterization, the analyses and regression equations presented in this paper directly apply to the estimation of design parameters. In the technical literature, there is no relationship between this test and design parameters in large-scale soil improvements with vertical gravel elements, as result, this study fills that gap.
- It has been demonstrated that the use of compacted granular fills (GC, SM, SC) in the first 3 to 4D of depth in RAP elements increases stiffness by 1.2 to 1.5 times on average compared to RAP in natural soils (clays or clayey silts) and increases the ultimate load capacity in long elements as those presented in this study.
- From the general behavior observed, RAP elements have higher load capacity and stiffness than SC elements by vibro replacement, with the former being more efficient. To illustrate this, the ratio between the ultimate load capacity of the element and its volume (kN/m^3) has been calculated, with the median for SC+NAT.SOIL being 70, RAP+NAT.SOIL being 100, and RAP+FILL being 110. As result, the RAP+FILL is 1.57 times more efficient than SC+NAT. SOIL. Cumulative frequency curves are shown in supplementary materials.
- A bi-normalized curves of head stress and deformation for vertical gravel elements were presented. These curves can be used to estimate the stress-deformation relationship, together with the empirical equations presented for q_{ult} in this study.

- In a subsequent paper, the deformation performance (magnitude and rate) of RAPs based on settlement plates data and results from three-dimensional finite element modeling will be presented to provide complementary interpretation of the results obtained in this paper.

DATA AVAILABILITY STATEMENT

Some or all data used during the study were provided by a third party. Direct requests for these materials may be made to the provider as indicated in the Acknowledgements.

ACKNOWLEDGEMENTS

To Interagua company for providing the load test information of RAP and settlement plate readings at the Northern WWTP, to GEOESTUDIOS company for providing the geotechnical information at Northern and Southern WWTP. The authors also thank the Public Water Company of Guayaquil EMAPAG for donating the load test information, CPTu, and gravel columns installed at the Southern WWTP.

DISCLAIMER

The vertical elements (SC) presented in this study were not designed or installed under the supervision, with authorization, or in compliance with Geopier's patented technology. The load tests on RAP elements were carried out under Geopier's supervision, while the load tests on SC were conducted independently.

NOTATION

a_{net}	net cone area
D	Diameter of the vertical gravel element
DSS	direct simple shear test
E_{50}	Secant deformation modulus at 50% of failure stress
FC%	fine content
Fr	normalized friction index
FOS	Factor of safety
f_s	shaft resistance of the cone
GM	geometric mean
Ic	soil behavior type index
PI	plasticity index
I_r	stiffness index
K_0	coefficient of lateral earth pressure

k_g	vertical stiffness of the vertical gravel element
kr	undisturbed soil permeability
ks	smear zone permeability
L	Vertical gravel element length
M	oedometric modulus
Np	bearing capacity factor
OCR	overconsolidation ratio
Qtn	normalized cone resistance
q_c	cone resistance
q_g	stress at the vertical gravel element head
q_s	soil matrix vertical stress
q_t	corrected cone resistance
q_{ult}	ultimate bearing capacity of the vertical gravel element
R_a	ratio of areas between improvement area and soil
R_s	ratio between gravel pile secant modulus and soil secant modulus
S	Vertical gravel element spacing
S'	smear zone diameter / gravel pile diameter
Su	undrained shear strength
ε_v	vertical strain
ϕ'	soil friction angle
ϕ_p	Vertical gravel element friction angle
25D	25 times the diameter
3D	3 times the diameter

SUPPLEMENTAL DATA

Figure S1-S3 and table S1 are available online in the ASCE Library (www.ascelibrary.org).

REFERENCES

Adalier, K., & Elgamal, A. (2004). Mitigation of liquefaction and associated ground deformations by stone columns. *Engineering Geology*, *72*(3–4), 275–291. https://doi.org/10.1016/j.enggeo.2003.11.001

Barksdale, R. D., & Bachus, R. C. (1983). *Design and construction of stone columns Rep. No. FHWA/RD 83/026*. Turner-Fairbank Highway Research Center.

Bergado, D. T., Asakami, H., Alfaro, M. C., & Balasubramaniam, A. S. (1991). Smear Effects of Vertical Drains on Soft Bangkok Clay. *Journal of Geotechnical Engineering*, *117*(10), 1509–1530. https://doi.org/10.1061/(ASCE)0733-9410(1991)117:10(1509)

Cadden, A., Gómez, J., Bruce, D., & Armour, T. (2004). Micropiles: Recent Advances and Future Trends. *Current Practices and Future Trends in Deep Foundations*, 140–165. https://doi.org/10.1061/40743(142)9

Datye, K. R. (1982). Settlement and bearing capacity of foundation system with stone columns. *Int. Symp. on Soil and Rock Improvement Techniques Including Geotextiles, Reinforced Earth, and Modern Piling Methods*.

Duncan, J. M., & Chang, C.-Y. (1970). Nonlinear Analysis of Stress and Strain in Soils. *Journal of the Soil Mechanics and Foundations Division*, *96*(5), 1629–1653. https://doi.org/10.1061/JSFEAQ.0001458

GEOESTUDIOS S.A. (2015). *Manual Práctico para la Caracterización Geológica, Geotécnica y Sísmica de la ciudad de Guayaquil*.

Girsang, C. H., Gutierrez, M. S., & Wissmann, K. J. (2004). Modeling of the Seismic Response of the Aggregate Pier Foundation System. *GeoSupport 2004*, 485–496. https://doi.org/10.1061/40713(2004)56

Halabian, A. M., & Shamsabadi, P. J. (2015). Numerical Modeling of the RAP Construction Process and Its Effects on RAP Behavior. *International Journal of Geomechanics*, *15*(5). https://doi.org/10.1061/(ASCE)GM.1943-5622.0000429

Han, J. (2015). Recent research and development of ground column technologies. *Proceedings of the Institution of Civil Engineers - Ground Improvement*, *168*(4), 246–264. https://doi.org/10.1680/grim.13.00016

Han, J., & Ye, S. L. (2002). A Theoretical Solution for Consolidation Rates of Stone Column-Reinforced Foundations Accounting for Smear and Well Resistance Effects. *International Journal of Geomechanics*, *2*(2), 135–151. https://doi.org/10.1061/(ASCE)1532-3641(2002)2:2(135)

Handy, R. L. (2001). Does Lateral Stress Really Influence Settlement? *Journal of Geotechnical and Geoenvironmental Engineering*, *127*(7), 623–626. https://doi.org/10.1061/(ASCE)1090-0241(2001)127:7(623)

Handy, R. L., & White, D. J. (2006). Stress Zones Near Displacement Piers: I. Plastic and Liquefied Behavior. *Journal of Geotechnical and Geoenvironmental Engineering*, *132*(1), 54–62. https://doi.org/10.1061/(ASCE)1090-0241(2006)132:1(54)

Hughes, J. M. O., & Withers, N. J. (1974). Reinforcing of soft cohesive soils with stone columns: 18F, 9R. GROUND ENGNG. V7, N3. *International Journal of Rock Mechanics and Mining Sciences & Geomechanics Abstracts*, *11*(11), 42–49.

Hughes, J. M. O., Withers, N. J., & Greenwood, D. A. (1975). A field trial of the reinforcing effect of a stone column in soil. *Géotechnique*, *25*(1), 31–44. https://doi.org/10.1680/geot.1975.25.1.31

Indraratna, B., Basack, S., & Rujikiatkamjorn, C. (2013). Numerical Solution of Stone Column–Improved Soft Soil Considering Arching, Clogging, and Smear Effects. *Journal of Geotechnical and Geoenvironmental Engineering*, *139*(3), 377–394. https://doi.org/10.1061/(ASCE)GT.1943-5606.0000789

Kondner, R. L. (1963). Hyperbolic Stress-Strain Response: Cohesive Soils. *Journal of the Soil Mechanics and Foundations Division*, *89*(1), 115–143. https://doi.org/10.1061/JSFEAQ.0000479

Kwong, H. K., Lien, B., & Fox, N. S. (2002). Stabilizing landslides using rammed aggregate piers. *Proc., 5th Malaysian Road Conf., Kuala Lumpur, Malaysia*.

Ladd, C. C., & Foott, R. (1974). New Design Procedure for Stability of Soft Clays. *Journal of the Geotechnical Engineering Division*, *100*(7), 763–786. https://doi.org/10.1061/AJGEB6.0000066

Lutenegger, A. J., & Adams, M. T. (1998). Bearing capacity of footings on compacted sand. *Fourth Intentational Conference on Case Histories in Geotechnical Engineering*, 1216–1224.

Mitchell, J. K. (1981). Soil improvement-state of the art report. *Proc., 11th Int. Conf. on SMFE*, *4*, 509–565.

Mohamedzein, Y. E.-A., & Al-Shibani, I. H. (2011). Performance of an embankment supported on soft soil reinforced by stone columns. *Proceedings of the Institution of Civil Engineers - Ground Improvement*, *164*(4), 213–224. https://doi.org/10.1680/grim.2011.164.4.213

Ng, K. S., & Tan, S. A. (2015). Simplified homogenization method in stone column designs. *Soils and Foundations*, *55*(1), 154–165. https://doi.org/10.1016/j.sandf.2014.12.012

Pal, S., & Deb, K. (2019). Effect of clogging of stone column on drainage capacity during soil liquefaction. *Soils and Foundations*, *59*(1), 196–207. https://doi.org/10.1016/j.sandf.2018.10.005

Paredes, J. (2020). *Evaluación de Parámetros Geotécnicos de los Depósitos de Suelo Ubicados en la llanura Aluvial y en el Complejo Deltaico Estuarino de Guayaquil (ECU), y Sectores Adyacentes de Daule, Samborondón y Durán, mediante ensayos in situ CPTu*. ESPOL.

Parra, J. R., Caskey, J. M., Marx, E., & Dennis, N. (2007). Stabilization of Failing Slopes Using Rammed Aggregate Pier Reinforcing Elements. *Soil Improvement*, 1–10. https://doi.org/10.1061/40916(235)21

Rayamajhi, D., Ashford, S. A., Boulanger, R. W., & Elgamal, A. (2016). Dense Granular Columns in Liquefiable Ground. I: Shear Reinforcement and Cyclic Stress Ratio Reduction. *Journal of Geotechnical and Geoenvironmental Engineering*, *142*(7). https://doi.org/10.1061/(ASCE)GT.1943-5606.0001474

Rayamajhi, D., Boulanger, R. W., Ashford, S. A., & Elgamal, A. (2016). Dense Granular Columns in Liquefiable Ground. II: Effects on Deformations. *Journal of Geotechnical and Geoenvironmental Engineering*, *142*(7). https://doi.org/10.1061/(ASCE)GT.1943-5606.0001475

Robertson, P. K. (2009). Interpretation of cone penetration tests — a unified approach. *Canadian Geotechnical Journal*, *46*(11), 1337–1355. https://doi.org/10.1139/T09-065

Robertson, P. K. (2012). The James K. Mitchell Lecture: Interpretation of in-situ tests–some insights. *Proc. 4th Int. Conf. on Geotechnical and Geophysical Site Characterization–ISC*, *4*, 3–24.

Shields, C. S., FitzPatrick, B. T., & Wissmann, K. J. (2004). Modulus Load Test Results for *Rammed Aggregate Piers* ™ in Granular Soils. *GeoSupport 2004*, 460–472. https://doi.org/10.1061/40713(2004)54

Studedlein, A. W., & Holtz, R. D. (2012). Analysis of Footing Load Tests on Aggregate Pier Reinforced Clay. *Journal of Geotechnical and Geoenvironmental Engineering*, *138*(9), 1091–1103. https://doi.org/10.1061/(ASCE)GT.1943-5606.0000677

Stuedlein, A. W., & Holtz, R. D. (2013). Bearing Capacity of Spread Footings on Aggregate Pier Reinforced Clay. *Journal of Geotechnical and Geoenvironmental Engineering*, *139*(1), 49–58. https://doi.org/10.1061/(ASCE)GT.1943-5606.0000748

Tai, P., & Zhou, C. (2019). Effects of Clogging on Settlement Predictions of Ground Improved with Stone Columns. *KSCE Journal of Civil Engineering*, *23*(9), 3889–3896. https://doi.org/10.1007/s12205-019-2414-y

Thompson, M. J., Wissmann, K. J., & Pham, H. T. (2009). Performance Monitoring of a Rammed Aggregate Pier Foundation Supporting a Mechanically Stabilized Earth Wall. *Journal of Performance of Constructed Facilities*, *23*(4), 244–250. https://doi.org/10.1061/(ASCE)CF.1943-5509.0000010

Thum, T. S., Yerro, A., Green, R. A., Ye, E., Saade, A., & Wissmann, K. (2021). Settlement Prediction of a RAP-Supported Footing in Liquefiable Soils Subjected to a Seismic Loading. *IFCEE 2021*, 430–439. https://doi.org/10.1061/9780784483411.041

Tiznado, C., Dashti, S., & Ledezma, C. (2021). Probabilistic Predictive Model for Liquefaction Triggering in Layered Sites Improved with Dense Granular Columns. *Journal of Geotechnical and Geoenvironmental Engineering*, *147*(10). https://doi.org/10.1061/(ASCE)GT.1943-5606.0002609

Vera-Grunauer, X. (2014). *Seismic Response of a Soft, High Plasticity, Diatomaceous Naturally Cemented Clay Deposit*. University of California Berkeley.

Vera-Grunauer, X., Lopez-Zhindon, S., Ordoñez-Rendon, J., & Chavez-Abril, M. A. (2019). Liquefaction case histories after the 2016 megathrust Pedernales earthquake in Ecuador. In *Earthquake Geotechnical Engineering for Protection and Development of Environment and Constructions* (pp. 805–820). CRC Press.

Vera-Grunauer, X., Wissmann, K. J., Smith, M., & Arroyo-Esqueda, J. (2017). Liquefaction Mitigation of Silty Sand and Sandy Silt Soils with Rammed Aggregate Piers. *SOCIEDAD MEXICANA DE INGENIERÍA GEOTÉCNICA A.C.*

Vesić, A. S. (1972). Expansion of Cavities in Infinite Soil Mass. *Journal of the Soil Mechanics and Foundations Division*, *98*(3), 265–290. https://doi.org/10.1061/JSFEAQ.0001740

White, D. J., Wissmann, K. J., Barnes, A., & Gaul, A. J. (2002). Embankment support: a comparison of stone column and rammed aggregate pier soil reinforcement. *Proceedings of the 55th Canadian Geotechnical and 3rd Joint IAH-CNC and CGS Groundwater Specialty Conferences*, 20–23.

Wissmann, K. J. (1999). Bearing capacity of Geopier-supported foundation systems. *Technical Bulletin*, *2*.

Wissmann, K. J., FitzPatrick, B. T., White, D. J., & Lien, B. H. (2002). Improving global stability and controlling settlement with Geopier soil reinforcing elements. *Proceedings of the 4th International Conference on Ground Improvement Techniques*, *8*, 26–28.

Zalachoris, G., Zekkos, D., Yerro, A., Bowers, G. A., & Wissmann, K. J. (2023). 3D Numerical Assessment of Rammed Aggregate Pier Performance under Dynamic Loading in Liquefiable Soils. *Journal of Geotechnical and Geoenvironmental Engineering*, *149*(3). https://doi.org/10.1061/JGGEFK.GTENG-10795

CERTIFICACIÓN DE REVISIÓN DE PROYECTO DE TITULACIÓN

Por medio de la presente, Yo Davide Besenzon Venegas, Coordinador del Programa de Maestría en Geotecnia de la Escuela Superior Politécnica del Litoral (ESPOL), certifico que:

Con fecha 16 de febrero de 2024, los estudiantes Jorge Andrés Badillo Coello y Alvaro Andrés Pazmiño Román con números de identificación 0926324930 y 0925982852, respectivamente, de la Cohorte 3, presentaron la propuesta de su tema de titulación al Comité Académico del programa. Posteriormente, con fecha 22 de abril de 2024, el Comité revisó y aprobó la propuesta mediante la resolución FICT-CA-GEOTEC-005-2024, cumpliendo con los requisitos establecidos para la aprobación del tema.

A partir de dicha aprobación, los estudiantes mantuvieron reuniones periódicas con el tutor designado, Xavier Fernando Vera Grunauer, para la elaboración y desarrollo de su proyecto de titulación, siguiendo los lineamientos establecidos por el programa. Con fecha 08 de mayo de 2024, los estudiantes presentaron y sustentaron su proyecto de titulación ante el tribunal evaluador asignado, cumpliendo con el proceso formal de evaluación académica.

Por lo tanto, en calidad de Coordinador del Programa de Maestría en Geotecnia, certifico que el trabajo de titulación denominado **"Evaluación y desempeño de pilas de agregado apisonado y columnas de grava en suelos blandos arcillosos"**, realizado por los estudiantes Jorge Andrés Badillo Coello y Alvaro Andrés Pazmiño Román con números de identificación 0926324930 y 0925982852, respectivamente, ha sido revisado y evaluado conforme a los lineamientos y estándares establecidos por el programa.

Debido a circunstancias externas, no ha sido posible obtener las firmas de los involucrados (estudiante, tutor(es) y/o evaluadores). No obstante, en calidad de Coordinador del Programa, certifico que el proyecto cumple con los requisitos académicos y ha sido revisado para su presentación y archivo institucional.

Atentamente,

Firmado electrónicamente por:
DAVIDE BESENZON
VENEGAS

M. Sc. Davide Besenzon Venegas
Coordinador de la Maestría en Geotecnia